

Coexistence of spin-glass and ferromagnetic order in the $\pm J$ Heisenberg spin-glass model

A. D. Beath and D. H. Ryan

Physics Department and Centre for the Physics of Materials, McGill University, 3600 University Street, Montreal, Quebec, Canada H3A 2T8

(Received 27 June 2007; published 7 August 2007)

Monte Carlo simulations of the bond-frustrated $\pm J$ Heisenberg model confirm the existence of a finite temperature spin-glass transition at $T_{SG}=0.220(5)$. Remarkably, this transition temperature is composition dependent, rising to $T_{SG}=0.25(1)$ by the ferromagnet–spin-glass boundary. Coexistence of ferromagnetic and spin-glass ordering is observed at low frustration levels for $T < T_{xy}$, and the composition dependence of this transition is also followed. The behavior we observe below T_{xy} agrees with both the mean field prediction and the experimental observations while being inconsistent with “re-entrance,” which demands a loss of ferromagnetic order. The complete phase diagram is presented.

DOI: 10.1103/PhysRevB.76.064410

PACS number(s): 75.10.Hk, 75.40.Cx, 75.40.Mg, 75.50.Lk

I. INTRODUCTION

Many partially frustrated ferromagnets undergo a second transition (at T_{xy}), below T_c , where spin-glass order appears to develop. This behavior is frequently misnamed “re-entrant” by analogy with re-entrant superconductors; however, it is clear that the ferromagnetic order is not lost when the spin-glass ordering occurs at T_{xy} ,¹⁻³ and the transition is certainly not re-entrant. The experimental signature of spin-glass order developing uniformly throughout the material in the plane perpendicular to the existing ferromagnetic order is an excellent match to behavior found in a mean field bond-frustrated Heisenberg model studied by Gabay and Toulouse⁴ (GT). However, identifying T_{xy} with the GT transition suffers due to the long held view that realistic, short range, three dimensional Heisenberg spin-glass models do not develop spin-glass order at finite temperatures.⁵⁻⁷ If the spin glass does not exist, then it cannot coexist with ferromagnetism.

This view of the spin glass has now been demonstrated to be incorrect. Recent work has shown that three dimensional Heisenberg spin-glass models with nearest neighbor interactions do indeed order at finite temperatures,⁸⁻¹⁰ contrary to conventional wisdom. These new findings open the possibility that the GT phase transition may also exist at finite temperatures and thus corresponds to the experimentally observed behavior at T_{xy} . Here, we report the results of our Monte Carlo studies of the spin glass and GT phases using the same techniques which have proved successful in prior studies of canonical spin glasses.⁸⁻¹¹ We confirm the existence of a finite temperature spin-glass transition in the $\pm J$ model and map out the composition dependence of T_{xy} , showing that it too occurs at finite temperatures. The phase diagram is shown in Fig. 1. We also find that the transition at T_{xy} marks the onset of spin-glass ordering that coexists transverse to the ferromagnetic order, in full agreement with both the predicted properties of the GT transition and experimental observations.

II. MODEL AND METHODS

The bond-frustrated Heisenberg model that we study here has the Hamiltonian $\mathcal{H} = -\sum_{\langle i,j \rangle} J_{ij} \mathbf{S}_i \cdot \mathbf{S}_j$, where the sum runs

over all pairs of nearest neighbor, unit vector, classical Heisenberg spins \mathbf{S}_i residing on a three dimensional simple cubic lattice of linear dimension L with periodic boundary conditions. The exchange interactions J_{ij} for spin-glass models are usually taken either from a Gaussian distribution with mean J_0 and unity variance,⁴⁻¹⁰ or, in our case, $a \pm J$ distribution¹¹⁻¹⁶ with probability

$$P(J_{ij} = +1) = 1 - x \text{ and } P(J_{ij} = -1) = x. \quad (1)$$

The interactions $J_{ij} = +1$ ($J_{ij} = -1$) correspond to ferromagnetic (antiferromagnetic) bonds, respectively. Our choice of the $\pm J$ distribution is motivated by the fact that for $x=0$, the model is free of both disorder and frustration and reduces to

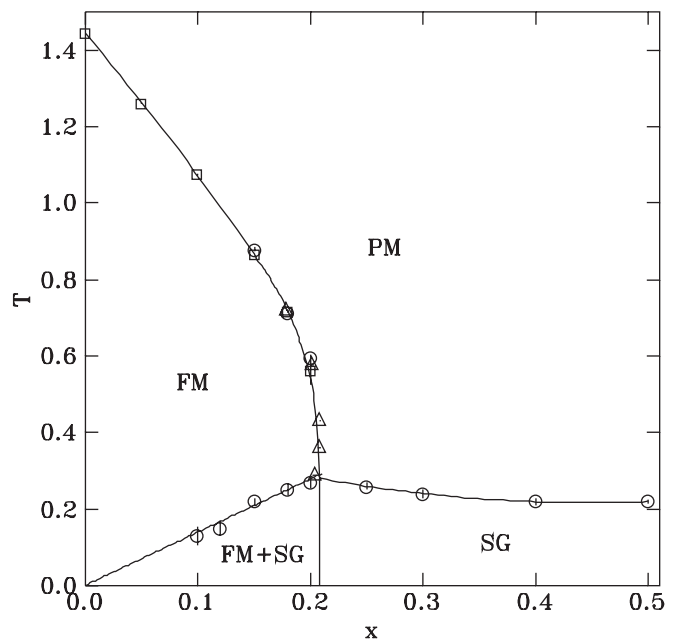


FIG. 1. Phase diagram of the $\pm J$ bond-frustrated Heisenberg model in three dimensions. PM refers to the paramagnetic phase, FM to the ferromagnetic phase, SG to the spin-glass phase, and FM+SG to the region where ferromagnetism and transverse spin-glass order coexist. Where error bars are not apparent, they are smaller than the symbol size.

the well understood Heisenberg ferromagnet with¹⁷ $T_C = 1.4429(1)$.

Adding exchange frustration ($x > 0$) to an otherwise ferromagnetic ($x = 0$) model leads to a reduction of T_C , and at the critical composition $x_c \sim 0.21$,^{13,14} ferromagnetism is lost. For $x_c < x \leq 0.5$, we observe spin-glass ordering at a finite T_{SG} . Our value at $x = 0.5$, $T_{SG} = 0.220(5)$, is greater than T_{SG} for the Gaussian model⁸⁻¹⁰ ($T_{SG} \sim 0.15$), in keeping with the trend observed in 3d nearest neighbor Ising spin-glass models¹¹ and consistent with some earlier predictions.^{15,16} One surprising result is that T_{SG} increases as x decreases. While the effect is small, T_{SG} is clearly composition dependent, contrary to the mean field predictions. As x decreases, the spin-glass transition meets the ferromagnetic phase boundary, and for $0 < x < x_c$, we observe the transverse spin-glass phase transition: ferromagnetic and spin-glass order coexist below a finite T_{xy} . All of the transitions are marked by a divergent correlation length and there is *no loss* of ferromagnetic order upon crossing T_{xy} , despite a rapid increase in the transverse spin-glass order parameter. Both T_{SG} and T_{xy} lie far below the mean field expectations,⁴ one reason why T_{SG} was not previously observed in Monte Carlo simulations.^{8,10}

To determine the phase diagram shown in Fig. 1, we have studied the model using a hybrid Monte Carlo algorithm that combines Metropolis with over-relaxation¹⁸ techniques, a method found to be efficient at equilibrating frustrated Heisenberg models.^{9,14,19,20} We begin each simulation in the paramagnetic state and anneal toward low temperatures. Following each Metropolis Monte Carlo update (one attempted spin update per lattice site), we use five over-relaxation updates^{14,18} which then comprise a single Monte Carlo step (MCS). We have previously shown that, for the system sizes studied here, $4 \leq L \leq 12$, the correlation times are drastically reduced by the inclusion of over-relaxation updates.¹⁴ To verify that our results are in equilibrium for each choice (T, L, x), we have calculated averages with logarithmically increasing numbers of MCS's, after discarding the same number of MCS's prior to the average. In the spin-glass regime of the phase diagram, we have used between 300 and 10^5 MCS's to compute thermal averages ($\langle \rangle$), followed by 100 bond configurations to compute disorder averages ($[\]$). In the ferromagnetic regime, we have used between 300 and 10^4 MCS's for thermal averaging and 500 bond configurations for disorder averaging. The bond configurations were chosen independently for each choice of the number of Monte Carlo steps, giving a total 400–600 bond configurations for $x > 0.2$ and 2000 bond configurations for $x \leq 0.2$.

The principal quantities we measure are wave vector dependent susceptibilities $\chi(\mathbf{k})$ from which we determine the correlation length^{8,9,11} using the definition

$$\xi = \frac{1}{2 \sin(|\mathbf{k}_{\min}|/2)} \left\{ \frac{[\langle \chi(0) \rangle]}{[\langle \chi(\mathbf{k}_{\min}) \rangle]} - 1 \right\}^{1/2}, \quad (2)$$

where $\mathbf{k}_{\min} = (2\pi/L, 0, 0)$ is the minimum wave vector allowed by our choice of boundary conditions. In a ferromagnetic phase, $\chi(\mathbf{k})$ is given by

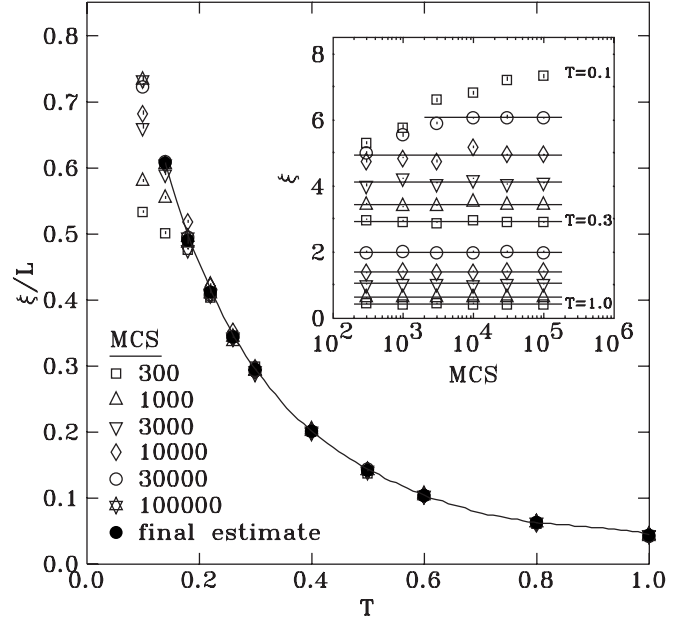


FIG. 2. ξ/L vs T for different numbers of MCSs used both prior to and during thermal averaging at $x = 0.5$, $L = 10$. Inset shows ξ vs MCS at various T . Horizontal lines in the inset show the regions used to determine our final averages. No time dependence is observed for $T \geq 0.18$. Where error bars are not apparent, they are smaller than the symbol size.

$$\chi(\mathbf{k}) = \beta L^3 \sum_{i,\mathbf{r}} \mathbf{S}_i \cdot \mathbf{S}_{i+\mathbf{r}} e^{i\mathbf{k} \cdot \mathbf{r}}, \quad (3)$$

where $\beta = 1/T$ is the inverse temperature and \mathbf{r} is the vector connecting spins \mathbf{S}_i and $\mathbf{S}_{i+\mathbf{r}}$. In addition, we measure the magnetization $\mathbf{m} = m_x + m_y + m_z$, where $m_\mu = N^{-1} \sum_i S_i^\mu$ and $\mu = x, y, z$ are Cartesian components of \mathbf{S}_i . The ferromagnetic order parameter is the scalar $m = (\sum_\mu m_\mu^2)^{1/2}$.

In the spin-glass phase, we simulate two replicas (1 and 2) with identical bonds and compute the spin-glass overlap tensor at site i , $q_{\mu\nu,i} = S_{i,1}^\mu S_{i,2}^\nu$. The wave vector dependent susceptibility is then given in terms of the overlap as

$$\chi(\mathbf{k}) = \beta N^{-1} \sum_{\mu,\nu} \sum_{i,\mathbf{r}} q_{\mu\nu,i} q_{\mu\nu,i+\mathbf{r}} e^{i\mathbf{k} \cdot \mathbf{r}}, \quad (4)$$

while the spin-glass order parameter is $q = (\sum_{\mu\nu} q_{\mu\nu}^2)^{1/2}$, with $q_{\mu\nu} = N^{-1} \sum_i q_{\mu\nu,i}$.

Where ferromagnetism exists, we define a transverse spin-glass overlap tensor $q_{\mu\nu,i}^\perp$, which is the overlap of spin components at site i perpendicular to the magnetization. In terms of $\mathbf{S}_i^\perp = \mathbf{S}_i - \mathbf{m} \cdot \mathbf{S}_i / m$, the transverse component of \mathbf{S}_i , we have $q_{\mu\nu,i}^\perp = S_{i,1}^{\mu,\perp} S_{i,2}^{\nu,\perp}$, where \mathbf{m} is the vector magnetization and m its magnitude for each replica. The definition of $\chi_\perp(\mathbf{k})$ is then the same as for the spin glass [Eq. (4)] with the replacement of $q_{\mu\nu,i}$ by $q_{\mu\nu,i}^\perp$. The transverse spin-glass order parameter is $q_{xy} = [\sum_{\mu\nu} (q_{\mu\nu}^\perp)^2]^{1/2}$, with $q_{\mu\nu}^\perp = N^{-1} \sum_i q_{\mu\nu,i}^\perp$.

III. RESULTS

In Fig. 2, we show $\xi(T, \text{MCS})$ for the canonical $\pm J$ Heisenberg spin glass ($x = 0.5$) with $L = 10$ (the smallest size

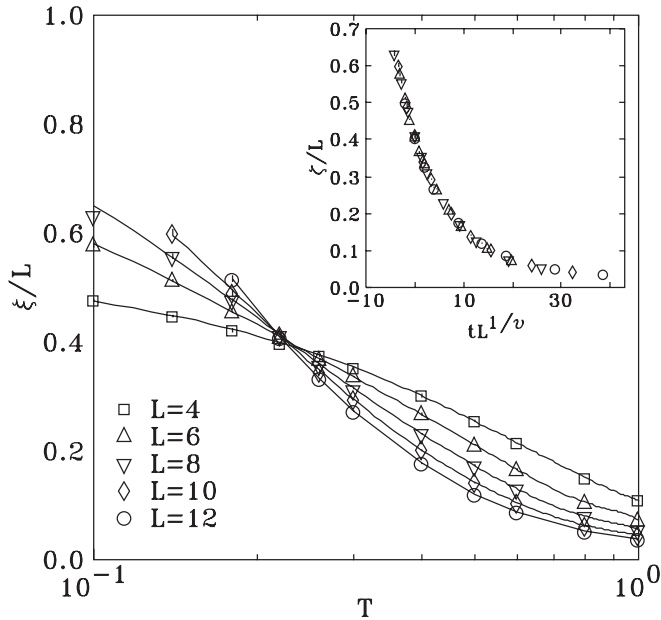


FIG. 3. Correlation length divided by system size, ξ/L , vs T for different L at $x=0.5$. A clear crossing is observed at $T_{SG}=0.220(5)$. Inset shows the scaling of ξ/L with $\nu=1.04$, and a reduced temperature $t=(T-T_{SG})/T_{SG}$, with $T_{SG}=0.22$. Where error bars are not apparent, they are smaller than the symbol size.

for which we observed a lack of equilibration). At high temperatures, ξ is independent of the number of MCS's. Only at low temperatures, $T < 0.18$, do we observe any dependence on the number of MCS's in our calculated ξ . The data at $T=0.14$ are obviously not equilibrated for either MCS=300 or MCS=1000 but are equilibrated for MCS ≥ 3000 . The lack of equilibration at $T=0.14$ for small MCS is revealed by the fact that the data remain correlated with the previous measurement at $T=0.18$, and the correlation disappears with increasing MCS. At $T=0.1$, we do not observe a clear convergence of ξ ; instead, ξ continues to increase with increasing MCS. We compute average values of ξ only for those results which have converged, indicated in the inset of Fig. 2 by solid lines. Our final estimates are shown in Fig. 2.

If a second order phase transition occurs at T_{SG} , then we expect $\xi \propto L^3$ for $T \ll T_{SG}$, $\xi \propto L$ for $T = T_{SG}$, and ξ constant for $T \gg T_{SG}$. Thus,^{8,11} a plot of ξ/L must cross at the transition temperature, splaying out both above and below. We have previously shown for the ferromagnetic transition that T_C found from the crossing of ξ/L curves agrees with other, more established, methods¹⁴ such as the crossing of the Binder cumulant. Our results for the canonical $\pm J$ Heisenberg spin glass ($x=0.5$) are shown in Fig. 3, and a clear crossing is observed at $T_{SG}=0.220(5)$. The crossing does not exhibit a noticeable shift with increasing L , except at $L=4$. This lack of large scaling corrections is not unexpected since, in the case of a Gaussian distribution of bonds, T_{SG} determined⁸ with $L \leq 12$ was found to agree with T_{SG} determined using much larger systems,^{9,10} $L \leq 32$. A fit to $\log(\xi)$ vs $\log(L)$ at $T=0.22$, omitting the $L=4$ data point, yields a slope $s=1.012(15)$, demonstrating that at $T=0.22$, we have $\xi \propto L$, confirming our assignment of T_{SG} . Our estimate, T_{SG}

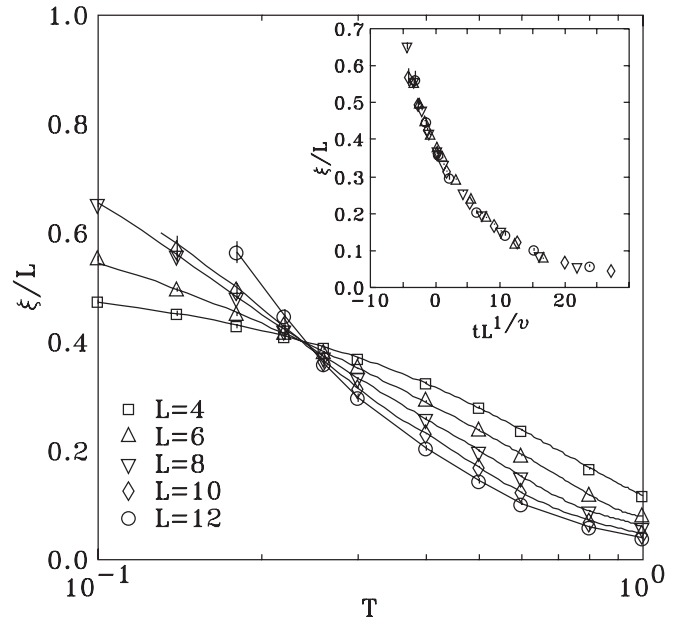


FIG. 4. Same as Fig. 3 except at the concentration $x=0.25$. A clear crossing is still observed, but it occurs at temperatures slightly above $T_{SG}(x=0.5)=0.22$, namely, $T_{SG}(x=0.25)=0.25(1)$. Inset shows the scaling of ξ/L with $\nu=1.04$, and a reduced temperature $t=(T-T_{SG})/T_{SG}$, with $T_{SG}=0.25$. Where error bars are not apparent, they are smaller than the symbol size.

$=0.220(5)$, is in agreement with other estimates of finite T_{SG} , namely, $T_{SG}=0.19(2)$ (Ref. 15) and $T_{SG}=0.22^{+0.0116}_{-0.04}$ who both used less established methods than we use here. In the inset of Fig. 3, we show the collapse of ξ/L vs T , with the expected finite size scaling form with $\nu=1.04$. We estimate ν by fitting the slope of $\xi(L)/L$ at T_{SG} , omitting the $L=4$ data point. Our estimate, $\nu=1.04(6)$, is also consistent with those of the $\pm J$ distribution^{15,16} and for the Gaussian distribution⁸ for the same range of system sizes.

It has been shown for the Gaussian model⁹ that the estimate of ν increases with L , and so the occurrence of a Kosterlitz-Thouless (KT)-like transition at T_{SG} , with $1/\nu=0$, cannot yet be ruled out.^{9,10} With the range of system sizes we use here, we also cannot determine whether a KT-like phase exists in the $\pm J$ spin-glass model below T_{SG} . However, a small value of $1/\nu$ would explain the lack of large scaling corrections we observe in the location of the crossing point of ξ/L , and so while estimates of T_{SG} are unlikely to change significantly with larger system sizes, the nature of the spin-glass phase may be more exotic. The nondivergent fluctuations observed in μ SR experiments³ at T_{SG} (and T_{xy}) could be related to KT-like transitions, while the divergent fluctuations seen at T_C represent true second order phase transitions.

As we decrease the amount of frustration,²⁰ moving left across the phase diagram toward the FM phase, we find that T_{SG} increases; by $x=0.25$, it is clear that $T_{SG}(x=0.25) > T_{SG}(x=0.5)$. To demonstrate this point, we calculate the slope s of $\log(\xi)$ vs $\log(L)$ at $T=0.22$ for different x . At $x=0.4$, we get $s=1.025(25)$, which remains consistent with $T_{SG}=0.22$. However, at $x=0.3$, we get $s=1.049(30)$, and at $x=0.25$, we get $s=1.055(13)$. This increase in s with decreas-

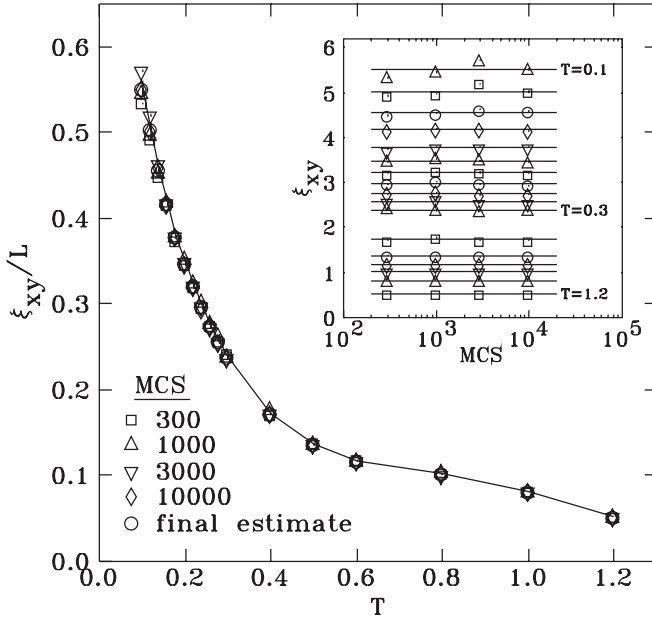


FIG. 5. ξ_{xy}/L vs T for different numbers of MCSs used both prior to and during thermal averaging at $x=0.15$, $L=10$. Inset shows ξ_{xy} vs MCS at various T . Horizontal lines in the inset show the regions used to determine our final averages. No time dependence is observed, even for as few as 300 MCSs. Where error bars are not apparent, they are smaller than the symbol size.

ing x at $T=0.22$ (T_{SG} for $x=0.4, 0.5$) indicates that $T_{SG}(x)$ is also increasing. In fact, the crossing point in the curves of ξ/L shows that by $x=0.25$, T_{SG} has moved to $0.25(1)$, as shown in Fig. 4. The spin-glass transition temperatures, which we determine by a weighted average of the six crossing points which occur for $L \geq 6$, are plotted in the phase diagram in Fig. 1 along with T_C determined in Ref. 14.

Turning to the transverse spin-glass phase existing below the ferromagnetic phase boundary, we show $\xi(T, \text{MCS})$ at $x=0.15$ with $L=10$ in Fig. 5. Unlike the pure spin glass, we find no time dependence in ξ , except for $L=12$ and $T < \frac{3}{4}T_{xy}$. Other quantities such as the internal energy, $[\langle q_{\perp} \rangle]$ and $[\langle m \rangle]$, in addition to having no MCS dependence, also show much smaller compositional fluctuations than ξ . Again, we make final estimates of $\xi(T)$ by averaging the data at a particular T , as indicated by solid lines in the inset of Fig. 5.

In Fig. 6, we show the crossing of ξ_{xy}/L for the five compositions studied here. Like the pure spin glasses, there is a clear crossing, but the $L=4$ data cross at a higher temperature than the others. The crossing point in ξ_{xy}/L , which we ascribe to the ordering of the transverse spin glass at T_{xy} , has a much more significant x dependence than that of T_{SG} . To an excellent approximation, T_{xy} is linear in x and passes through the origin. A fit to the form $T_{xy} = a + bx$ yields $a = 0.00(4)$ and $b = 1.39(25)$, consistent with T_{xy} vanishing at $x=0$. Furthermore, as shown in the inset of Fig. 6, there is a notable increase in ξ_{xy} upon crossing T_C due to a softening of the transverse ferromagnetic modes. We note that while there is a rapid increase in $[\langle q_{xy} \rangle]$ below T_{xy} , we do not observe any loss of ferromagnetic order: The spin-glass and ferromag-

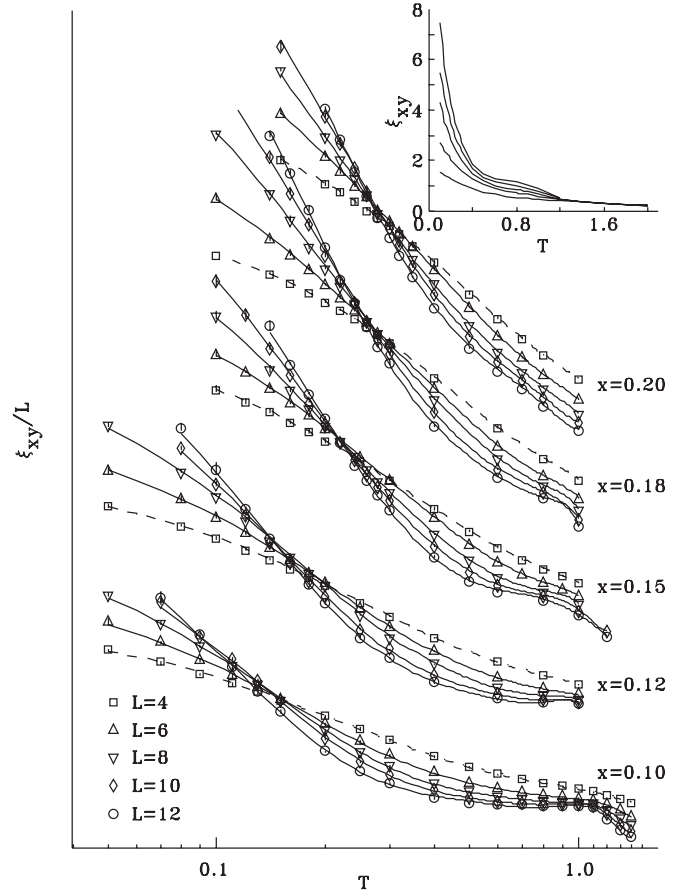


FIG. 6. Crossing of the ξ_{xy}/L curves for $L=4, 6, 8, 10$, and 12 for concentrations $x=0.20, 0.18, 0.15$, and 0.12 and $x=0.10$ (curves $x=0.10$ have been shifted to fit plotting area). Solid lines through $L > 4$ data show clear crossings, while the dashed line through the $L=4$ data crosses at higher T . Inset shows ξ_{xy} for $x=0.15$, which shows a nondivergent increase at T_C prior to T_{xy} . Where error bars are not apparent, they are smaller than the symbol size.

netic order coexist below T_{xy} . This behavior is fully consistent with both the GT phase⁴ and experiments on partially frustrated ferromagnets¹⁻³ where spin-glass order is found transverse to the magnetization below T_{xy} .

In the mean field GT phase diagram, T_C , T_{xy} , and T_{SG} merge at a multicritical point. Our phase diagram confirms this prediction although the location of the multicritical point is somewhat uncertain as the functional forms of the three phase boundaries are not known. Based on several types of fits, we conservatively estimate the location of the multicritical point to be $(x_{cri}, T_{cri}) = (0.21(1), 0.29(2))$.

IV. CONCLUSIONS

In summary, we have studied the phase diagram of the $\pm J$ Heisenberg spin-glass model in three dimensions with nearest neighbor interactions. We find all of the phases predicted by GT, including the mixed phase where spin-glass order and ferromagnetism coexist. We find that T_{SG} is composition dependent, contrary to the mean field prediction. Our results indicate that T_{xy} extrapolates to zero at $x=0$, which implies

that for even infinitesimal amounts of frustration, the model has two transitions, namely, ferromagnetic and transverse spin-glass transitions. Furthermore, we have located the multicritical point where T_C , T_{SG} , and T_{xy} merge. Our phase diagram for a realistic spin-glass model with short range inter-

actions demonstrates that the phases found in the mean field theory of Gabay and Toulouse survive at finite temperatures in three dimensions and that the behavior observed in experiments on partially frustrated ferromagnets is found in a simple spin-glass model.

-
- ¹D. H. Ryan, *Recent Progress in Random Magnets* (World Scientific, Singapore, 1992).
- ²D. H. Ryan, Z. Tun, and J. M. Cadogan, *J. Magn. Magn. Mater.* **177-181**, 57 (1998).
- ³D. H. Ryan, J. M. Cadogan, and J. van Lierop, *Phys. Rev. B* **62**, 8638 (2000).
- ⁴M. Gabay and G. Toulouse, *Phys. Rev. Lett.* **47**, 201 (1981).
- ⁵J. A. Olive, A. P. Young, and D. Sherrington, *Phys. Rev. B* **34**, 6341 (1986).
- ⁶J. R. Banavar and M. Cieplak, *Phys. Rev. Lett.* **48**, 832 (1982).
- ⁷W. L. McMillan, *Phys. Rev. B* **31**, 342 (1985).
- ⁸L. W. Lee and A. P. Young, *Phys. Rev. Lett.* **90**, 227203 (2003).
- ⁹I. Campos, M. Cotallo-Aban, V. Martín-Mayor, S. Perez-Gaviro, and A. Tarancón, *Phys. Rev. Lett.* **97**, 217204 (2006).
- ¹⁰L. W. Lee and A. P. Young, *Phys. Rev. B* **76**, 024405 (2007).
- ¹¹H. G. Ballesteros, A. Cruz, L. A. Fernández, V. Martín-Mayor, J. Pech, J. J. Ruiz-Lorenzo, A. Tarancón, P. Téllez, C. L. Ullod, and C. Ungil, *Phys. Rev. B* **62**, 14237 (2000).
- ¹²J. R. Thomson, H. Guo, D. H. Ryan, M. J. Zuckermann, and M. Grant, *J. Appl. Phys.* **69**, 5231 (1991); *Phys. Rev. B* **45**, 3129 (1992).
- ¹³F. Matsubara, T. Iyota, and S. Inawashiro, *J. Phys. Soc. Jpn.* **60**, 4022 (1991).
- ¹⁴A. D. Beath and D. H. Ryan, *J. Appl. Phys.* **97**, 10A506 (2005).
- ¹⁵S. Endoh, F. Matsubara, and T. Shirakura, *J. Phys. Soc. Jpn.* **70**, 1543 (2001).
- ¹⁶T. Nakamura and S. Endoh, *J. Phys. Soc. Jpn.* **71**, 2113 (2002).
- ¹⁷K. Chen, A. M. Ferrenberg, and D. P. Landau, *Phys. Rev. B* **48**, 3249 (1993).
- ¹⁸M. Creutz, *Phys. Rev. D* **36**, 515 (1987).
- ¹⁹J. L. Alonso, A. Tarancón, H. G. Ballesteros, L. A. Fernández, V. Martín-Mayor, and A. Muñoz Sudupe, *Phys. Rev. B* **53**, 2537 (1996).
- ²⁰A. D. Beath and D. H. Ryan, *Phys. Rev. B* **73**, 214445 (2006).